J Petrol Explor Prod Technol (2014) 4:457–469
DOI 10.1007/s13202-014-0103-4

ORIGINAL PAPER - PRODUCTION ENGINEERING

Identification of pitfalls in PVT gas condensate modeling using modified black-oil formulations

Pichit Vardcharragosad · Abraham Duplaa · Luis F. Ayala H.

Received: 13 September 2013 / Accepted: 11 January 2014 / Published online: 11 February 2014

Abstract A black-oil (BO) PVT model is a fluid characterization formulation that represents multi-component reservoir hydrocarbons as a binary mixture (i.e., two pseudo-components: "surface gas" and "stock tank oil"). The BO PVT model is widely used in the petroleum industry because it is relatively simple compared to fully compositional modeling in which all or most components are independently accounted for. Since computational complexity increases nearly exponentially with number of components used in the characterization, there always remains a strong incentive to embracing the simplified black oil (binary) characterization as long as the fluid phase behavior allows it. When representing a complex system with this simplified model, a number of limitations arising from its simplicity may exist. In this study, these limitations are highlighted by performing phase behavior simulations for a gas condensate fluid. Rigorous calculations of standard (BO) PVT properties (B_o, B_g, R_s, and R_v) of a the gas condensate reservoir of choice are performed through a series of flash calculations at the prescribed reservoir fluid depletion path. The study demonstrates that the BO PVT model violates the species material balance principle as reservoir pressure depletes while conserving overall mass. This violation can lead to significant errors when coupling the BO PVT model with tank material balance-based techniques. The simulation test case indicates that these models will significantly and consistently underestimate oil formation volume factor (B_o) and solution gas oil ratio (R_s) due to the shortcomings of the BO PVT model.

P. Vardcharragosad · A. Duplaa · L. F. Ayala H. (✉)
John and Willie Leone Family Department of Energy and Mineral Engineering, The Pennsylvania State University, University Park, PA, USA
e-mail: lfay@psu.edu

Keywords Black Oil · PVT Analysis · Gas Condensates · Natural Gas Reservoirs

List of symbols

B_g	Gas formation volume factor (RB/MSCF)
B_o	Oil formation volume factor (RB/STB)
c_i	Overall molar fraction of i-th component
f_{ng}	Molar fraction of gas phase
f_{nl}	Molar fraction of liquid phase
G	Amount of surface gas (MSCF)
G_{fg}	Amount of surface gas remaining in reservoir gas (MSCF)
G_{fo}	Amount of surface oil remaining in reservoir oil (MSCF)
G_p	Cumulative gas production (MSCF)
N	Amount of stock tank oil (STB)
N_{fg}	Amount of stock tank oil remaining in reservoir gas (STB)
N_{fo}	Amount of stock tank oil remaining in reservoir oil (STB)
N_p	Cumulative oil production (STB)
n_{EG}	Mole of Excess Gas (lbmol)
n_g	Mole of reservoir gas inside PVT cell after excess gas removal (lbmol)
n_{g+EG}	Mole of reservoir gas inside PVT cell before excess gas removal (lbmol)
n_o	Mole of reservoir oil inside PVT cell (lbmol)
n_T	Mole of reservoir fluid (gas and oil) inside PVT cell (lbmol)
R_s	Solution gas–oil ratio (SCF/STB)
R_v	Volatilized oil–gas ratio (STB/MMSCF)
V_{EG}	Excess gas volume (RB)
V_g	Reservoir gas volume after excess gas removal (RB)

V_{g+EG} Reservoir gas volume before excess gas removal (RB)
V_o Reservoir oil volume (RB)
V_T PVT cell volume (RB)
x_g Molar fraction of surface gas in reservoir oil
x_o Molar fraction of stock tank oil in reservoir oil
y_g Molar fraction of surface gas in reservoir gas
y_o Molar fraction of stock tank oil in reservoir gas

Abbreviations

BO Black-oil
CVD Constant volume depletion
MM Million
PVT Pressure–volume–temperature
RB Reservoir barrel
SCF Standard cubic feet
STB Stock tank barrel
WTA Walsh–Towler algorithm

Subscript

EG Excess gas
fg Free gas
fo Free oil
g Gas
i Component *i*
j Pressure level *j*
o Oil
T Total

Introduction

A black-oil (BO) PVT model is a fluid characterization model that represents multi-component reservoir hydrocarbons in only two pseudo-components, "surface gas" and "stock tank oil" (Walsh and Lake 2003; Whitson and Brule 2000). "Surface gas" is a pseudo-component consisting of hydrocarbons in the reservoir that remain in the gas phase at standard conditions. "Stock tank oil" is the other pseudo-component consisting of hydrocarbons in the reservoir that remain in the oil phase at standard conditions. This BO PVT model is widely used in the petroleum industry because it is relatively simple compared to a fully compositional model. The modified BO PVT model relies on the definition of four standard properties: oil formation volume factor (B_o), gas formation volume factor (B_g), solution gas–oil ratio (R_s), and volatilized oil–gas ratio (R_v). Figure 1 is graphical representation of the definitions of these properties. B_o represents the ratio between the amount of reservoir oil (V_o) and stock tank oil (N_{fo}) produced from that reservoir oil, while B_g represents the ratio between the amount of reservoir gas (V_g) and surface gas (G_{fg}) produced from that reservoir gas. R_v denotes solubility of stock tank oil (N_{fg}) in surface gas (G_{fg}) produced

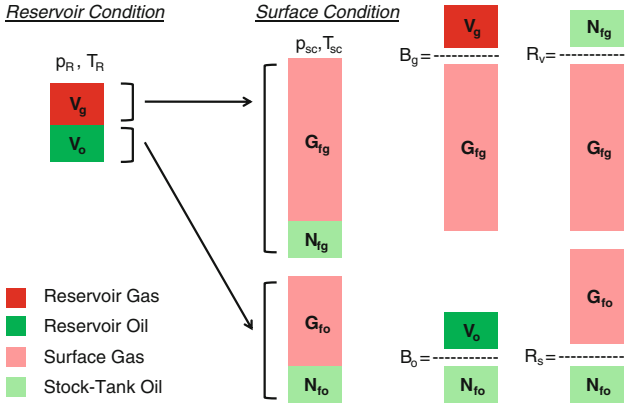

Fig. 1 Graphical representation of standard PVT properties (modified from Walsh and Lake 2003)

from the same reservoir gas, while R_s denotes solubility of surface gas (G_{fo}) in stock tank oil (N_{fo}) produced from the same reservoir oil. Classical BO PVT models only allowed the "surface gas" pseudo-component to be part of both the reservoir gas and oil phases, but did not allow the "stock tank oil" pseudo-component to partake in the reservoir gas ($R_v = 0$). BO models that incorporate the calculation of R_v are considered "modified" BO PVT models, while for the classical BO models, $R_v = 0$.

Modified BO models are routinely used to model all five conventional reservoir fluid types: black oils, volatile oils, retrograde gases, wet gases and dry gases (McCain 1990; Walsh and Lake 2003). In this study, the analysis of retrograde gases is of interest. In gas condensate, retrograde gas condensate, or retrograde gas reservoirs, the reservoir fluid may be initially a single vapor phase. Upon volumetric depletion, the reservoir is subjected to isothermal expansion process at constant reservoir volume. Once reservoir pressure drops below the dew point, a condensate phase is formed. This liquid hydrocarbon is usually immobile and can cause variability in factors that ultimately could affect recovery factor (Walsh and Lake 2003). Excess gas resulted from the expansion process will be released to surface in the form of produced oil and natural gas. They will then be treated at surface production facilities, which are designed to satisfy all sale specifications. In this study, the depletion behavior of gas condensate will be studied using modified BO models and fully compositional flash calculations. Flash calculations can predict amount, composition, and properties of each phase based on pressure, temperature, overall composition, and physical properties of pure components. In this paper, gas compressibility factor is calculated using Peng and Robinson Equation of State (Peng and Robinson 1976). Vapor–liquid equilibrium is evaluated by implementing material balance (Rachford and Rice 1952) and equilibrium thermodynamic considerations (Coat 1985). Fluid property

correlations include a volume-translation technique for density adjustment by Jhaveri and Youngren (1988), gas viscosity by Lee et al. (1966), and liquid viscosity by Lohrenz et al. (1964). Phase stability is analyzed using Michelson's algorithm (1982).

Simulating the standard (BO) PVT properties

In this study, the standard (BO) PVT properties for a gas condensate reservoir are rigorously simulated by performing a series of flash calculations of the gas condensate fluid at the prescribed conditions through a constant volume depletion (CVD) path. The CVD process mimics the depletion mechanism of gas condensate reservoirs as described earlier. The algorithm consists of pre-calculation steps and nine calculation steps. Its graphical representation and complete calculation procedure are described in Appendix B. The detailed procedure can be found in Vardcharragosad (2011). The Walsh–Towler's method (Walsh and Lake 2003) and Whitson–Torp method (Whitson and Torp 1983) are used to analyze the resulting PVT data. This study is based on the reservoir fluid characterization and input data detailed in Appendix A. Pre-calculation starts by assuming there is 1.0 MMSCF of Gas-Equivalent inside the PVT cell of study charged with the reservoir fluid of study at dew point conditions. Dew point pressure, the PVT cell volume, surface gas (G), and stock tank oil (N) at the dew point are determined using flash calculations. The main calculation begins by dropping the pressure inside the PVT cell to the new pressure level then evaluating amount and properties of each phase inside the PVT cell. The new PVT cell volume at the new pressure level is calculated and the amount of excess reservoir gas is removed to bring the PVT cell back to its initial. The amount and properties of G and N then can be extracted from the remaining reservoir gas and oil inside the PVT cell after excess gas removal is evaluated. Then, B_o, B_g, R_s, and R_v values are calculated using the definitions presented in Fig. 1. This calculation process will be repeated at the new pressure level until the pressure inside the PVT cell reaches the abandonment pressure condition.

Based on this protocol, standard (BO) PVT properties are calculated for the gas condensate fluid described in Appendix A. Reservoir initial pressure is 4,000 psia and temperature 300 °F. Fluid dew point pressure is 3,224 psia at the stated reservoir temperature. The simulated reservoir gas properties (B_g and R_v) and the simulated reservoir oil properties (B_o and R_s) are displayed in Figs. 2 and 3, respectively. The behavior of these properties is similar to the actual behavior observed from Anschutz Rance East rich-gas condensate reservoir (Walsh and Lake 2003). B_g values monotonically increase with decreasing reservoir

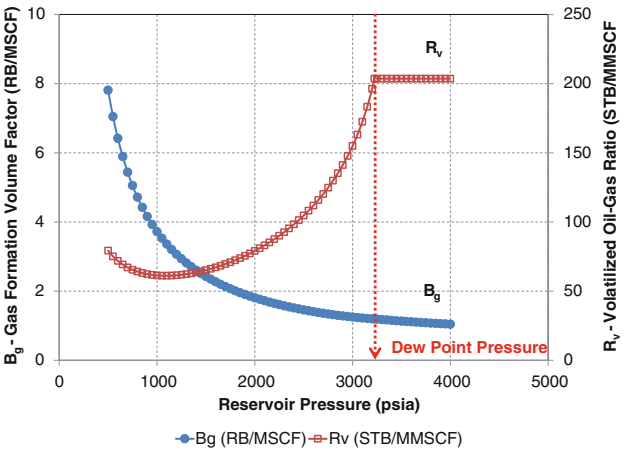

Fig. 2 Simulated B_g and R_v of gas condensate

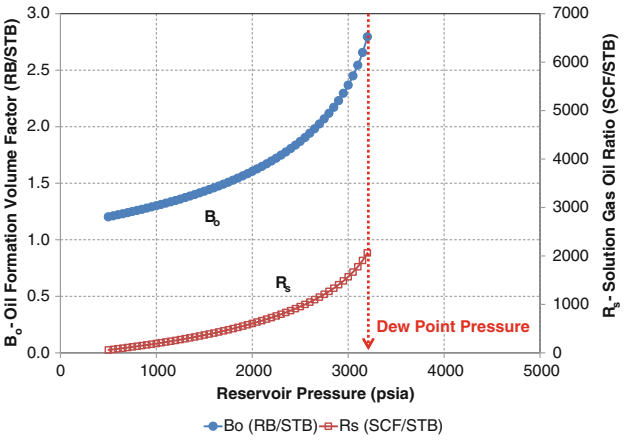

Fig. 3 Simulated B_o and R_s of gas condensate

pressure because of fluid expansion. R_v values remain constant above the dew point because there is no composition change in reservoir gas; however, they decrease with decreasing reservoir pressure below the dew point due to retrograde condensation. B_o and R_s are not defined above the dew point. As reservoir pressure goes below the dew point, B_o and R_s values decrease with depleting reservoir pressure because of solution gas liberation.

Identification of pitfalls

While our simulations have started with a total amount of 1.0 MMSCF of Gas-Equivalent at the dew point, total amount of G ("surface gas") and N ("stock tank oil") found in the reservoir gas, reservoir oil, and cumulative production at every reservoir depletion step can be straightforwardly calculated from above results. This information is depicted in Figs. 4 and 5. Figure 4 shows that the amount of surface gas remaining in the reservoir gas (G_{fg}) decreases as reservoir pressure decreases because

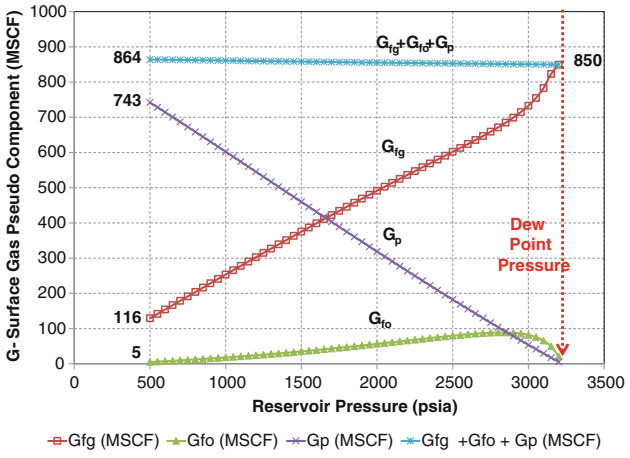

Fig. 4 Amount of surface gas (G_{fg}, G_{fo}, and G_p)

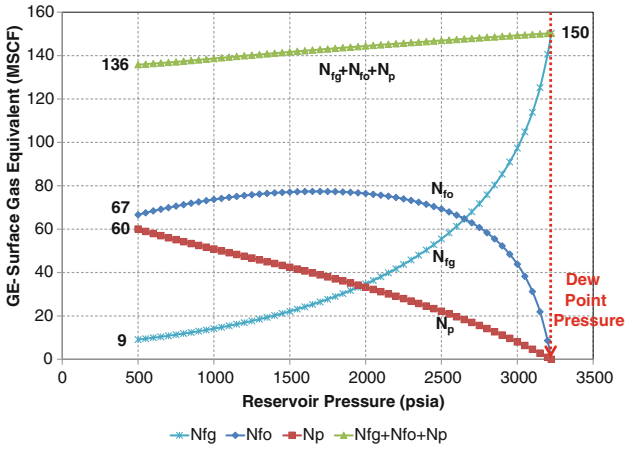

Fig. 5 Amount of stock tank oil (N_{fg}, N_{fo}, and N_p)

reservoir gas is continuously removed. The amount of surface gas remaining in reservoir oil (G_{fo}) is zero at the dew point. Its amount increases, reaches a maximum, and then decreases as reservoir pressure continues to decrease below the dew point. This reversing trend is mainly dominated by the amounts of reservoir oil, which in turn, drive the combined effect of retrograde condensation and solution gas liberation. Cumulative gas production (G_p), which is the amount of surface gas recovered from the production of excess gas from the PVT cell, increases with decreasing reservoir pressure due to accumulating hydrocarbon production.

In Fig. 5, the amount of stock tank oil remaining in reservoir gas (N_{fg}) decreases with decreasing reservoir pressure due to production and retrograde condensation of reservoir gas. The amount of stock tank oil remaining in reservoir oil (N_{fo}) is zero at the dew point. Its amount increases, reaches a maximum, and then decreases as reservoir pressure continues decreasing below the dew point. Similar to G_{fo}, this reversing trend is dominated by the

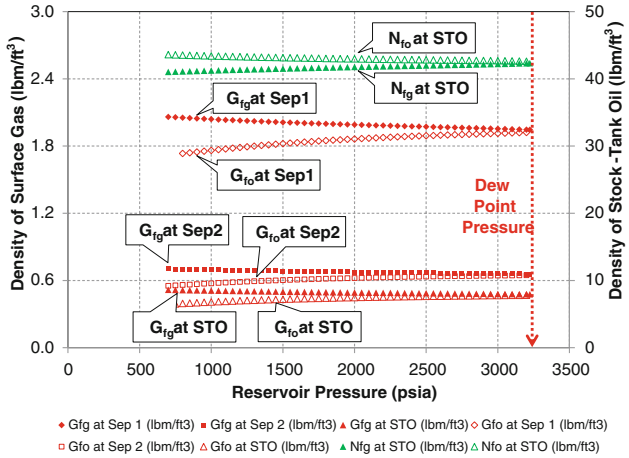

Fig. 6 Density of surface gas and stock tank oil

changing amounts of reservoir oil during depletion. Cumulative oil production (N_p), the amount of stock tank oil recovered from the production of the excess gas from the PVT cells, increases as reservoir pressure decreases due to accumulating hydrocarbon production.

Material balance conservation needs to be considered for each of the pseudo-components to understand further implications of the BO PVT model. Since G must be conserved, the sum of the surface gas in reservoir gas, reservoir oil, and cumulative gas production, ($G_{fg} + G_{fo} + G_p$) must equal the amount of surface gas pseudo-component in reservoir gas (G_{fg}) initially available at dew point conditions. Yet, Fig. 4 shows that the sum of G increases with decreasing reservoir pressure. Similarly, the sum of stock tank oil in reservoir gas, reservoir oil, and cumulative oil production ($N_{fg} + N_{fo} + N_p$) decreases with decreasing reservoir pressure, as shown in Fig. 5. This violation in the conservation principle of pseudo-components can be attributed to the assumptions of the pseudo-component model, which implies that each pseudo-component behaves as a pure component (constant composition, same independent of depletion) while in reality each pseudo-component is a mixture in itself. Each pseudo-component is a multi-component mixture whose composition is susceptible to change during depletion. In particular, by lumping all mixture components into two pseudo-components (light and heavy), the effect of the intermediate components in the depletion process is being neglected.

Reservoir gas and oil phase compositions continuously change throughout the reservoir life cycle because of retrograde condensation, solution gas liberation, and immobile condensate drop out inside the reservoir. Separator conditions of first stage separator, second stage separator, and stock tank also result in different compositions of the pseudo-components recovered from said surface

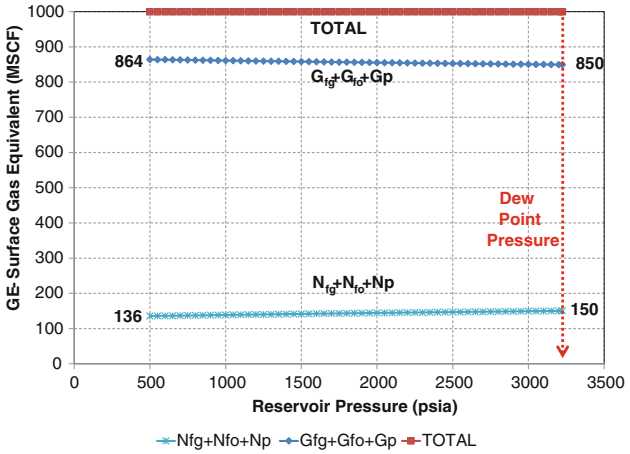

Fig. 7 Gas-equivalent of surface gas and stock tank oil

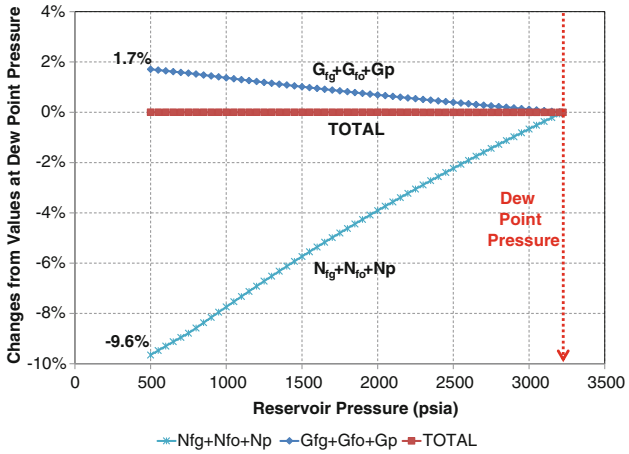

Fig. 8 Percentage differences in gas-equivalent of surface gas and stock tank oil

separators. Compositional changes in pseudo-components can be observed from the change in their densities. Figure 6 displays the calculated densities of surface gas and stock tank oil pseudo-components recovered at different separators. As reservoir pressure decreases, densities of G_{fg} and N_{fo} exhibit increasing trends while densities of G_{fo} and N_{fg} exhibit decreasing trends. These trends clearly support the fact that properties of the pseudo-components always change. Thus, any calculation based on conservation principles applied to two pseudo-components may lead to significant error.

Further analysis was carried out by converting stock tank oil pseudo-components (N_{fg}, N_{fo}, and N_p) into gas-equivalent units. The total amount of stock tank oil ($N_{fg} + N_{fo} + N_p$), surface gas ($G_{fg} + G_{fo} + G_p$), and their sum are calculated and plotted in Fig. 7. These results indicate that the total amount of fluid remains constant and equal to 1.0 MMSCF, which is the original amount of fluid at dew point conditions. The figure illustrates that the BO PVT model honors overall (total) material balance, but it cannot honor species material balance conservation for each of the two pseudo-species. Figure 8 shows the associated percentage material balance error for total amount of stock tank oil ($N_{fg} + N_{fo} + N_p$), surface gas ($G_{fg} + G_{fo} + G_p$) relative to their initial amounts at dew point condition. The trend in both figures is for total amount of surface gas ($G_{fg} + G_{fo} + G_p$) to *increase* and for total amount stock tank oil ($N_{fg} + N_{fo} + N_p$) to *decrease* with decreasing pressure. This effect is due to the tendency of liquid intermediates to further volatilize as pressure decreases—an effect fully ignored by the two-pseudo-component (light, heavy) BO PVT formulation which requires each pseudo-component to remain at fixed compositions (i.e., with the same amount of intermediates regardless of pressure). In the next section, we explore the impact that lack of species material balance conservation can have on the calculation of PVT properties typically used in BO PVT material balance calculations.

Impact on standard (BO) PVT property prediction

The limitation of the BO PVT model in violating the species material balance principal could lead to significant errors when pairing the BO PVT model with species material balance-based techniques such as Walsh–Towler algorithm (Walsh and Towler 1995; Walsh and Lake 2003). The Walsh–Towler algorithm is a practical method to determine B_o, B_g, R_s, and R_v on the basis of CVD experimental results. In a CVD experiment, properties of the immobile reservoir oil left inside the PVT cell are not usually reported. When the Walsh–Towler algorithm is used to simulate reservoir oil-related properties such as B_o and R_s, reservoir oil properties are estimated assuming stock-tank oil species conservation at all times.

To demonstrate the impact of lack of species material balance conservation can have on the calculation of PVT properties using the BO PVT model, CVD experimental results are rigorously simulated based on input data and calculation procedure in Appendixes A and C, respectively. The simulated CVD results are shown in Appendix D. Subsequently, B_o, B_g, R_v, and R_s are calculated based on those simulated CVD results using Walsh–Towler algorithm. Detailed calculations for the Walsh–Towler algorithm can be found in Appendix E. Results are shown in Table 1. In Table 1, the standard (BO) PVT properties calculated directly from a series of rigorous flash calculations (left) are compared to those calculated from the Walsh–Towler algorithm (right). Percent errors observed by implementing the Walsh–Towler algorithm, compared to those using rigorous flash calculations, are presented in

Table 1 Comparison of standard PVT property calculations

Pressure (psia)	Rigorous flash calculations				BO PVT property prediction algorithm (Walsh–Towler)			
	B_o (RB/STB)	B_g (RB/MSCF)	R_s (SCF/STB)	R_v (STB/MMSCF)	B_o (RB/STB)	B_g (RB/MSCF)	R_s (SCF/STB)	R_v (STB/MMSCF)
3,224		1.20		204		1.20		204
3,000	2.37	1.25	1,570	155	2.33 (−1 %)	1.25	1,529 (−3 %)	155
2,750	2.07	1.34	1,207	125	2.02 (−2 %)	1.34	1,152 (−5 %)	125
2,500	1.87	1.46	954	105	1.82 (−3 %)	1.46	887 (−7 %)	105
2,250	1.72	1.61	761	90	1.66 (−4 %)	1.61	684 (−10 %)	90
2,000	1.60	1.81	605	79	1.53 (−4 %)	1.81	518 (−14 %)	79
1,750	1.51	2.07	476	71	1.43 (−5 %)	2.07	379 (−20 %)	71
1,500	1.43	2.43	366	65	1.34 (−6 %)	2.43	259(−29 %)	65
1,250	1.36	2.94	272	62	1.27 (−7 %)	2.94	154 (−43 %)	62
1,000	1.30	3.72	191	61	1.20 (−8 %)	3.72	61 (−68 %)	61
750	1.25	5.05	121	65	1.14 (−9 %)	5.05	−22 (−118 %)	65
500	1.20	7.81	59	78	1.08 (−10 %)	7.81	−96 (−261 %)	78

parentheses. As shown, the Walsh–Towler algorithm consistently underestimates B_o and R_s, and the error becomes more significant at lower pressure. However, it does not impact B_g and R_v calculations. These trends are caused due to the lack of species material balance conservation in the BO PVT model demonstrated in the previous section.

BO PVT property prediction algorithms, such as the Walsh–Tower algorithm, are built around the presumably valid assumption that the total amount of stock tank oil ($N_{fg} + N_{fo} + N_p$) and total amount of surface gas ($G_{fg} + G_{fo} + G_p$) would be conserved throughout the depletion process. In reality, because of the shortcomings of the BO pseudo-component formulation which ignores intermediate component effects, total amount of surface gas ($G_{fg} + G_{fo} + G_p$) actually *increases* with decreasing pressure (see Figs. 4, 7) and total amount stock tank oil in the system ($N_{fg} + N_{fo} + N_p$) *decreases* with decreasing pressure (see Figs. 5, 7).

As a consequence of this, and because N_{fg} and N_p values are derived directly from the CVD data, any lack of compliance with stock tank oil material balance conservation is automatically (yet unintendedly) absorbed by N_{fo}. At high pressures, the differences in actual and calculated total stock tank oil are relatively small compared to N_{fo}; thus, the error is small and can be neglected. However, lower pressures exhibit greater differences in total stock tank oil and, therefore, the error can become significant. The imposition that total stock tank oil ($N_{fg} + N_{fo} + N_p$) should remain the same during depletion (while actually decreasing with pressure depletion due to BO PVT shortcomings) invariably leads to a consistent overestimation of N_{fo}. This, in turn, leads to a consistent underestimation of B_o—as per its definition shown in Fig. 1 and as illustrated in Table 1.

The consequences of the lack of compliance with species material balance by the BO PVT formulation become especially exacerbated during the calculation of R_s, where physically negated negative values can be found (see Table 1). This is caused by the overestimation of N_{fo}, described above, compounded with an underestimation of G_{fo}. BO PVT property prediction algorithms preserve total amount of total surface gas ($G_{fg} + G_{fo} + G_p$), in spite of it being an *increasing* quantity as pressure depletes due to the volatilization of liquid intermediates. This leads to a consistent underestimation of G_{fo} based on such material balance constraint that uses G_{fg} and G_p values independently obtained from CVD data. The combination of underestimated G_{fo} values with overestimated N_{fo} values can translate into seriously underestimated R_s, (see R_s definition in Fig. 1 and calculated values in Table 1, with estimation errors higher than 200 %). This underestimation can be so severe that negative values of R_s can be found at low pressures—for this case, for pressures below 800 psia. At pressures below 800 psia, the sum of G_{fg} and G_p becomes higher than total surface gas ($G_{fg} + G_{fo} + G_p$) at dew point pressure leading to negative R_s values. It should be noted that N_{fo} and G_{fo} values do not participate in the calculation of B_g and R_v (see Fig. 1), and thus errors in their estimation do not impact B_g and R_v calculations.

Differences between properties calculated from direct flash calculation (Appendix B) and species material balance-based techniques have been also reported by Izgec and Barrufet (2005). Izgec and Barrufet calculated the standard (BO) PVT properties from flash calculations using Whitson–Torp algorithm (1983), and used Coats Procedure (1985) to calculate properties using a species material balance-based method. Coats also indicated the discrepancy caused by representing complex hydrocarbon

mixtures with the black-oil model, by comparing well-stream compositions calculated from numerical simulators. Coats also described the same effect using a local (grid block-scaled) compositional simulation.

Concluding remarks

Standard BO PVT properties of a gas condensate reservoir have been rigorously simulated based on hypothetical reservoir fluid and prescribed reservoir and surface production conditions to provide insight into the limitations of black-oil PVT formulations. Simulation results demonstrated that species material balance conservation of surface gas and stock tank oil pseudo-components can be violated by the BO PVT model, while still honoring overall material balance. The limitation stems from assumption inherent to the pseudo-component model, which requires the composition of every pseudo-component to remain the same regardless of pressure. The violation of the species material balance principle by the BO PVT model leads to significant errors in standard BO PVT property estimations when techniques that rely on species material balance statements are used. A case example shows that calculated reservoir oil-related PVT properties such as oil formation volume factor (B_o) and solution gas–oil ratio (R_s) using BO PVT property prediction algorithms can be significantly underestimated due to the BO PVT model limitations.

Appendix A

Reservoir fluid characterization and input data

This appendix presents all input data used to calculate the results reported in this study (Tables 2, 3, 4, 5).

Appendix B

Simulating standard PVT properties using the phase behavior model

This appendix summarizes the calculation procedure for simulating standard PVT properties calculation (B_o, B_g. R_s, and R_v) using a thermodynamic phase behavior model. Figure 9 depicts the graphical representation of terms used in the equations below. The phase behavior model is a computer code used to calculate quantities and properties of each phase of hydrocarbon mixture based on given composition, pressure, and temperature data. Further details of the simulation procedure and phase behavior model can be found in Vardcharragosad (2011).

Table 2 Reservoir and separator conditions

	Pressure (psia)	Temperature (°F)
Reservoir condition	4,000	300
1st stage separator	500	90
2nd stage separator	150	65
Stock tank condition	100	60

Pre-calculation

First, dew point pressure of reservoir hydrocarbon was determined by implementing a series of phase stability analysis. Then, the moles of initial reservoir fluid inside PVT cell (n_T or $n_{T,0}$) was calculated based on 1.0 MMSCF of gas equivalent using Eq. 1. The volume of the PVT cell (V_T), initial amount of surface gas (G) and stock tank oil (N) were evaluated based on the amount of initial reservoir fluid (n_T) at dew point conditions, using Eqs. 2–4.

$$n_T\{\text{lbmol}\} = \frac{p_{sc}\{\text{psia}\} \times G_e\{\text{ft}^3\}}{10.73\{(\text{psi} - \text{ft}^3)/(R - \text{lbmol})\} \times T_{sc}\{R\}} \quad (1)$$

$$V_T\{\text{ft}^3\} = \frac{n_T\{\text{lbmol}\} \times \text{MW}_T\{\text{lbm/lbmol}\}}{\rho_T\{\text{lbm/ft}^3\}} \quad (2)$$

$$G\{\text{SCF}\} = (y_g \times n_T\{\text{lbmol}\}) \times 379.56\{\text{SCF/lbmol}\} \quad (3)$$

$$N\{\text{STB}\} = \frac{(y_o \times n_T\{\text{lbmol}\}) \times \text{MW}_o^{\text{STO}}\{\text{lbm/lbmol}\}}{\rho_o^{\text{STO}}\{\text{lbm/ft}^3\} \times \{5.615\,\text{ft}^3/\text{bbl}\}} \quad (4)$$

Step 1: Find $n_{g+EG,j}$ and $n_{o,j}$

Amount of moles of reservoir gas before the removal of excess gas ($n_{g+EG,j}$) and moles of reservoir oil ($n_{o,j}$) at every pressure level j were calculated based on remaining moles of reservoir fluid (gas and oil) after excess gas removal at every pressure level $j-1$ ($n_{T,j-1}$) and the overall molar fraction of gas phase at every pressure level j ($f_{ng,j}^{PVT}$), using Eq. 5 and Eq. 6.

$$n_{g+EG,j}\{\text{lbmol}\} = n_{T,j-1}\{\text{lbmol}\} \times f_{ng,j}^{PVT} \quad (5)$$

$$n_{o,j}\{\text{lbmol}\} = n_{T,j-1}\{\text{lbmol}\} \times \left(1 - f_{ng,j}^{PVT}\right) \quad (6)$$

Step 2: Find $V_{g+EG,j}$ and $V_{o,j}$

The volume reservoir gas before the removal of the excess gas ($V_{g+EG,j}$) and the volume of reservoir oil ($V_{o,j}$) at every pressure level j were determined from moles of each

Table 3 Reservoir fluid composition and physical properties of pure components

Component	Mole fraction	Critical pressure (psia)	Critical temperature (R)	Acentric factor	Molecular weight (lbm/lbmol)	Critical volume (ft^3/lbm)
N_2	0.0223	493.10	227.49	0.0372	28.0134	0.0510
C_1	0.6568	666.40	343.33	0.0104	16.0430	0.0988
C_2	0.1170	706.50	549.92	0.0979	30.0700	0.0783
C_3	0.0587	616.00	666.06	0.1522	44.0970	0.0727
i-C_4	0.0127	527.90	734.46	0.1852	58.1230	0.0714
n-C_4	0.0168	550.60	765.62	0.1995	58.1230	0.0703
i-C_5	0.0071	490.40	829.10	0.2280	72.1500	0.0679
n-C_5	0.0071	488.60	845.80	0.2514	72.1500	0.0675
n-C_6	0.0138	436.90	913.60	0.2994	86.1770	0.0688
n-C_{10}	0.0832	305.20	1,112.00	0.4898	142.2850	0.0679
CO_2	0.0045	1,071.00	547.91	0.2667	44.0100	0.0344

Table 4 Binary interaction coefficients of pure components

δ_{ij}'s	N_2	C_1	C_2	C_3	i-C_4	n-C_4	i-C_5	n-C_5	n-C_6	n-C_{10}	CO_2
N_2	0.0000	0.0250	0.0100	0.0900	0.0950	0.0950	0.1000	0.1100	0.1100	0.1100	0.0000
C_1	0.0250	0.0000	0.0050	0.0100	0.0350	0.0250	0.0500	0.0300	0.0300	0.0450	0.1050
C_2	0.0100	0.0050	0.0000	0.0050	0.0000	0.0100	0.0100	0.0100	0.0200	0.0200	0.1300
C_3	0.0900	0.0100	0.0050	0.0000	0.0000	0.0000	0.0150	0.0020	0.0100	0.0050	0.1250
i-C_4	0.0950	0.0350	0.0000	0.0000	0.0000	0.0000	0.0050	0.0050	0.0050	0.0050	0.1200
n-C_4	0.0950	0.0250	0.0100	0.0000	0.0000	0.0000	0.0050	0.0050	0.0050	0.0050	0.1150
i-C_5	0.1000	0.0500	0.0100	0.0150	0.0050	0.0050	0.0000	0.0000	0.0000	0.0000	0.1150
n-C_5	0.1000	0.0300	0.0100	0.0020	0.0050	0.0050	0.0000	0.0000	0.0000	0.0000	0.1150
n-C_6	0.1100	0.0300	0.0200	0.0100	0.0050	0.0050	0.0000	0.0000	0.0000	0.0000	0.1150
n-C_{10}	0.1250	0.0450	0.0200	0.0050	0.0050	0.0050	0.0000	0.0000	0.0000	0.0000	0.1150
CO_2	0.0000	0.1050	0.1300	0.1250	0.1200	0.1150	0.1150	0.1150	0.1150	0.1150	0.0000

Source Nagy and Shirkovskiy (1982)

phase ($n_{g+EG,j}$ and $n_{o,j}$)calculated from Step 1, using Eq. 7 and Eq. 8.

$$V_{g+EG,j}\{RB\} = \frac{n_{g+EG,j}\{lbmol\} \times MW_{g,j}^{PVT}\{lbm/lbmol\}}{\rho_{g,j}^{PVT}\{lbm/ft^3\} \times \{5.615\,ft^3/bbl\}} \quad (7)$$

$$V_{o,j}\{RB\} = \frac{n_{o,j}\{lbmol\} \times MW_{o,j}^{PVT}\{lbm/lbmol\}}{\rho_{o,j}^{PVT}\{lbm/ft^3\} \times \{5.615\,ft^3/bbl\}} \quad (8)$$

Step 3: Find $V_{g,j}$ and $V_{EG,j}$

The volume of reservoir gas after excess gas removal at pressure level j ($V_{g,j}$) and the volume of excess gas at pressure level j ($V_{EG,j}$) were calculated from the volume of PVT cell (V_T) and the output volumes from Step 2, using Eq. 9 and Eq. 10.

$$V_{g,j}\{RB\} = V_T\{RB\} - V_{o,j}\{RB\} \quad (9)$$

$$V_{EG,j}\{RB\} = V_{g+EG,j}\{RB\} - V_{g,j}\{RB\} \quad (10)$$

Table 5 Volume translation coefficient of pure components

Component	Si for Peng–Robinson EOS
N_2	−0.19270
C_1	−0.15950
C_2	−0.11340
C_3	−0.08630
i-C_4	−0.08440
n-C_4	−0.06750
i-C_5	−0.06080
n-C_5	−0.03900
n-C_6	−0.00800
n-C_{10}	0.06550
CO_2	−0.08170

Step 4: Find $n_{g,j}$ and $n_{EG,j}$

The remaining moles of reservoir gas after excess gas removal at every pressure level j ($n_{g,j}$) and moles of excess gas which are removed at pressure level j ($n_{EG,j}$) were then

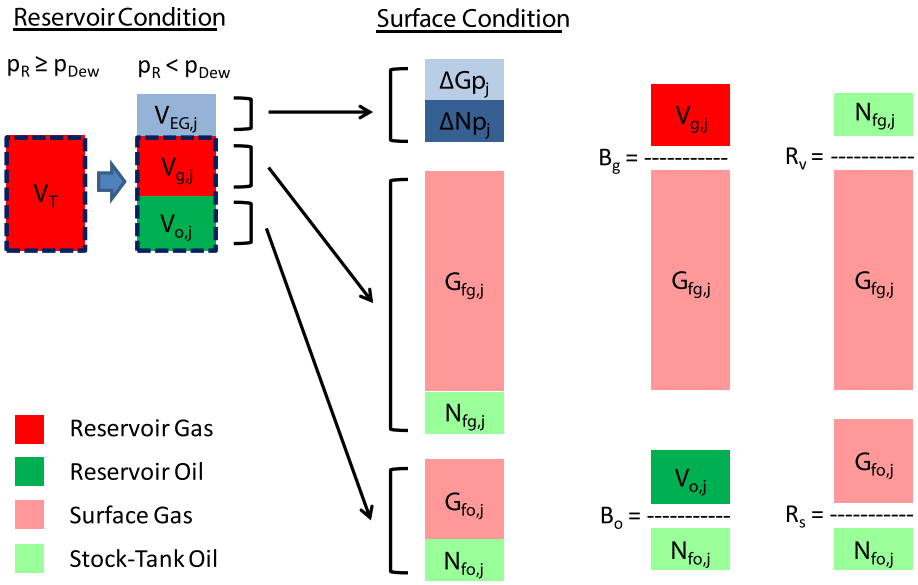

Fig. 9 Graphical representation of the data used in standard PVT properties simulation

Table 6 Pressure–volume relations of reservoir fluid at 300 °F (constant composition expansion)

Pressure (psia)	Relative volume	Z-factor
4,000	0.8720	0.929
3,750	0.9062	0.905
3,500	0.9465	0.882
3,250	0.9945	0.860
3,224[a]	1.0000	0.858

[a] Dew point pressure

computed from the volumes in Step 3, using Eq. 11 and Eq. 12.

$$n_{g,j}\{\text{lbmol}\} = \frac{V_{g,j}\{\text{RB}\} \times \rho_{g,j}^{\text{PVT}}\{\text{lbm/ft}^3\} \times \{5.615\,\text{ft}^3/\text{bbl}\}}{\text{MW}_{g,j}^{\text{PVT}}\{\text{lbm/lbmol}\}} \tag{11}$$

$$n_{\text{EG},j}\{\text{lbmol}\} = \frac{V_{\text{EG},j}\{\text{RB}\} \times \rho_{g,j}^{\text{PVT}}\{\text{lbm/ft}^3\} \times \{5.615\,\text{ft}^3/\text{bbl}\}}{\text{MW}_{g,j}^{\text{PVT}}\{\text{lbm/lbmol}\}} \tag{12}$$

Step 5: Find $y_{g,j}$ and $y_{o,j}$

The molar fractions of surface gas ($y_{g,j}$) and stock tank oil ($y_{o,j}$) in the reservoir gas at every pressure level j were calculated by performing series of flash calculation on the reservoir gas through designed production separator conditions, using Eq. 13 and Eq. 14.

$$y_{g,j} = 1 - \left(f_{\text{nl},g,j}^{\text{Sep1}} \times f_{\text{nl},g,j}^{\text{Sep2}} \times f_{\text{nl},g,j}^{\text{STO}}\right) \tag{13}$$

$$y_{o,j} = f_{\text{nl},g,j}^{\text{Sep1}} \times f_{\text{nl},g,j}^{\text{Sep2}} \times f_{\text{nl},g,j}^{\text{STO}} \tag{14}$$

Table 7 Retrograde condensation during constant volume depletion at 300 °F

Pressure (psia)	Retrograde liquid volume (% of hydrocarbon pore space)
3,224	0.0
3,000	12.4
2,750	15.2
2,500	15.7
2,250	15.6
2,000	15.1
1,750	14.5
1,500	13.9
1,250	13.1
1,000	12.4
750	11.6
500	10.7

Step 6: Find $G_{fg,j}$ and $N_{fg,j}$

The volumes of surface gas ($G_{fg,j}$) and stock tank oil ($N_{fg,j}$) in reservoir gas at pressure level j were calculated from the remaining mole of reservoir gas ($n_{g,j}$) and the molar fractions of surface gas ($y_{g,j}$) and stock tank oil ($y_{o,j}$) in reservoir gas, using Eq. 15 and Eq. 16.

$$G_{fg,j}\{\text{SCF}\} = (y_{g,j} \times n_{g,j}\{\text{lbmol}\}) \times 379.56\{\text{SCF/lbmol}\} \tag{15}$$

$$N_{fg,j}\{\text{STB}\} = \frac{(y_{o,j} \times n_{g,j}\{\text{lbmol}\}) \times \text{MW}_{o,g,j}^{\text{STO}}\{\text{lbm/lbmol}\}}{\rho_{o,g,j}^{\text{STO}}\{\text{lbm/ft}^3\} \times \{5.615\,\text{ft}^3/\text{bbl}\}}. \tag{16}$$

Table 8 Depletion study at 300 °F

Compositions of the produced wellstreams: mole percent												
	Reservoir pressure (psia)											
	3,224	3,000	2,750	2,500	2,250	2,000	1,750	1,500	1,250	1,000	750	500
Component												
N2	2.23	2.22	2.21	2.19	2.16	2.12	2.08	2.02	1.94	1.85	1.71	1.49
C1	65.68	65.53	65.23	64.78	64.17	63.36	62.30	60.91	59.04	56.46	52.67	46.60
C2	11.70	11.70	11.68	11.66	11.63	11.58	11.50	11.38	11.19	10.90	10.40	9.49
C3	5.87	5.88	5.89	5.91	5.93	5.96	5.98	6.00	6.00	5.97	5.87	5.58
i-C4	1.27	1.27	1.28	1.29	1.30	1.31	1.33	1.35	1.37	1.39	1.41	1.39
n-C4	1.68	1.68	1.70	1.71	1.73	1.75	1.78	1.82	1.86	1.90	1.94	1.95
i-C5	0.71	0.71	0.72	0.73	0.74	0.76	0.78	0.81	0.84	0.89	0.94	0.99
n-C5	0.71	0.71	0.72	0.73	0.75	0.76	0.79	0.82	0.86	0.91	0.97	1.04
n-C6	1.38	1.39	1.41	1.44	1.48	1.53	1.60	1.70	1.82	1.98	2.21	2.54
n-C10	8.32	8.45	8.72	9.12	9.67	10.42	11.43	12.78	14.65	17.35	21.50	28.59
CO2	0.45	0.45	0.45	0.45	0.44	0.44	0.43	0.43	0.42	0.40	0.38	0.34
Z-factor												
Gas phase	0.86	0.86	0.87	0.87	0.88	0.88	0.89	0.90	0.91	0.92	0.93	0.95
Two-phase	0.86	0.85	0.84	0.84	0.83	0.82	0.81	0.80	0.79	0.76	0.73	0.67

Step 7: Find $x_{g,j}$ and $x_{o,j}$

The molar fractions of surface gas ($x_{g,j}$) and stock tank oil ($x_{o,j}$) in the reservoir oil at every pressure level j were calculated by performing series of flash calculation on the reservoir oil through designed production separator conditions, using Eq. 17 and Eq. 18.

$$x_{g,j} = 1 - \left(f_{nl,o,j}^{Sep1} \times f_{nl,o,j}^{Sep2} \times f_{nl,o,j}^{STO}\right) \tag{17}$$

$$x_{o,j} = f_{nl,o,j}^{Sep1} \times f_{nl,o,j}^{Sep2} \times f_{nl,o,j}^{STO} \tag{18}$$

Step 8: Find $G_{fo,j}$ and $N_{fo,j}$

The volumes of surface gas ($G_{fo,j}$) and stock tank oil ($N_{fo,j}$) in reservoir oil at pressure level j were calculated from the remaining mole of reservoir oil ($n_{o,j}$) and the molar fractions of surface gas ($x_{g,j}$) and stock tank oil ($x_{o,j}$) in reservoir oil, using Eq. 19 and Eq. 20.

$$G_{fo,j}\{\text{SCF}\} = (x_{g,j} \times n_{o,j}\{\text{lbmol}\}) \times 379.56\{\text{SCF/lbmol}\} \tag{19}$$

$$N_{fo,j}\{\text{STB}\} = \frac{(x_{o,j} \times n_{o,j}\{\text{lbmol}\}) \times \text{MW}_{o,o,j}^{STO}\{\text{lbm/lbmol}\}}{\rho_{o,o,j}^{STO}\{\text{lbm/ft}^3\} \times \{5.615\text{ft}^3\text{/bbl}\}} \tag{20}$$

Step 9: Find $n_{T,j}$ and $c_{i,j}$

The remaining moles of reservoir fluid ($n_{T,j}$) and overall composition ($c_{i,j}$) inside PVT cell at pressure level j after gas removal were updated by removing moles of excess gas ($n_{EG,j}$) and re-calculating overall composition using Eq. 21 and Eq. 22.

$$n_{T,j} = n_{T,j-1} - n_{EG,j} \tag{21}$$

$$c_{i,j} = \frac{x_{i,j} \times n_{o,j} + y_{i,j} \times n_{g,j}}{n_{T,j}} \tag{22}$$

After completing all nine steps outlined above for the given pressure level, the results obtained can be used to calculate the standard PVT properties. All applicable unit conversion factors must be checked and adjusted properly. The calculation process is systematically repeated for all j pressure levels until all reported data in the CVD report have been considered and abandonment conditions have been reached.

Appendix C

Simulating CVD and CCE testing results using a phase behavior model

This appendix summarizes the calculation procedure for simulating constant volume depletion (CVD) and constant composition expansion (CCE) testing results using the phase behavior model. Since this appendix can be thought of as a continuation of Appendix B, many of the values found in Appendix B are used for further calculations.

Table 9 Calculated cumulative recovery during depletion

Cumulative recovery per 1.0 MMSCF of original fluid												
	Initial in place	Reservoir pressure (psia)										
		3,224	3,000	2,750	2,500	2,250	2,000	1,750	1,500	1,250	1,000	750	500
Stock tank oil (BBL)	173.0	0.0	8.4	16.3	23.2	29.2	34.7	39.7	44.3	48.7	53.1	57.7	63.1
1st Sep gas (MSCF)	819.0	0.0	52.6	114.5	178.8	245.2	313.2	382.5	452.5	522.8	593.0	662.4	730.2
2nd Sep gas (MSCF)	26.3	0.0	1.3	2.5	3.6	4.6	5.6	6.4	7.2	8.0	8.8	9.6	10.7
Stock tank gas (MSCF)	4.3	0.0	0.2	0.4	0.6	0.8	0.9	1.0	1.2	1.3	1.4	1.6	1.7

Step 1: Find Z_j (above dew point pressure)

The Peng–Robinson equations of state (PR-EOS) are used to calculate Z-factor at pressure level j (Z_j). The dew point pressure is previously determined in pre-calculation step of Appendix B. Above the dew point, composition of reservoir fluid is constant. Thus, Z-factor at reservoir pressure higher the dew point can be calculated based on reservoir pressure level j (p_j), reservoir temperature (T_R) and original reservoir fluid composition (c_i), and other physical properties of pure components. Reservoir pressure level (p_j) will be varied pressure from initial reservoir pressure to the dew point pressure.

$$Z_j = f\left(p_j, T_R, c_i, p_{ci}, T_{ci}, \omega_i, \text{BIP}\right) \tag{23}$$

Step 2: Find $V_{rel,j}$

The relative volume at pressure level j ($V_{rel,j}$) is calculated from Z-factor (Z_j) in Step 1, their corresponding pressures (p_j), Z-factor at the dew point (Z_{dew}) and the dew point pressure (p_{dew}), using Eq. 24:

$$V_{rel,j} = \left(\frac{Z_j}{P_j\{\text{psia}\}}\right) \Big/ \left(\frac{Z_{dew}}{p_{dew}\{\text{psia}\}}\right) \tag{24}$$

Step 3: Find $V_{ret,j}$

Retrograde liquid volume at desired pressure level j ($V_{ret,j}$) required the volume of reservoir oil ($V_{o,j}$) and total volume of the PVT cell (V_T) from Appendix B. Retrograde Liquid volume are calculated using Eq. 25:

$$V_{ret,j}\{\%\} = \left(\frac{V_{o,j}\{\text{RB}\}}{V_T\{\text{RB}\}}\right) \times 100 \tag{25}$$

Step 4: Find produced wellstreams compositions ($c_{i,j}$)

Mole percent of each component in produced wellstreams at desired pressure level j is calculated using Eq. 22.

Step 5: Find $Z_{g,j}$ below dew point pressure

Z-factor of gas at desired pressure level j ($Z_{g,j}$) below the dew point are calculated using PR-EOS. The calculation will be very similar to the calculation in Step 1, except the original reservoir composition (c_i) is replaced by gas composition at desired pressure level j ($y_{i,j}$) calculated in Appendix B.

$$Z_j = f\left(p_j, T_R, y_{i,j}, p_{ci}, T_{ci}, \omega_i, \text{BIP}\right) \tag{26}$$

Step 6: Find $Z_{2p,j}$

Two-phase Z-factor is defined as a ratio between the real fluid volume and the volume when that fluid behaves like ideal gas. The real fluid volume is equal to total volume of PVT cell (V_T) determined in Appendix B. Ideal gas volume ($V_{ideal,j}$) at pressure level j is calculated based on the remaining mole of reservoir fluid ($n_{T,j}$) using Eq. 27. Two-phase Z-factor ($Z_{2p,j}$) at pressure level j is calculated based on total PVT cell volume (V_T) and the ideal gas volume ($V_{ideal,j}$) using Eq. 28:

$$V_{ideal,j}\{\text{RB}\} = \frac{n_{T,j} \times \left\{10.73159 \frac{\text{ft}^3 \times \text{psi}}{\text{lbmol} \times R}\right\} \times T_R\{R\}}{p_j\{\text{psia}\} \times \{5.615\,\text{ft}^3/\text{bbl}\}} \tag{27}$$

$$Z_{2p,j} = \frac{V_T\{\text{RB}\}}{V_{ideal,j}\{\text{RB}\}} \tag{28}$$

Appendix D

Simulated CVD testing results

This appendix presents simulated constant volume depletion testing results based on input data in Appendix A and calculation procedure in Appendix C. Note that the calculation results are based on 1.0 MMSCF of Gas-Equivalent at the dew point conditions (Tables 6, 7, 8, 9).

Appendix E

Simulating standard PVT properties using Walsh and Towler algorithm

This appendix presents standard PVT properties calculation based on simulated CVD testing results in Appendix D and Walsh and Towler algorithm (Walsh and Lake 2003) (Tables 10, 11, 12).

Table 10 Pre-calculation results

G_e (MSCF-eq)	G (MSCF)	N (STB)	V_T (RB)
1,000.0	849.55	173.01	1,018.66

Table 11 Input from simulated CVD results

j	Pres (psia)	G_{p1} (MSCF)	G_{p2} (MSCF)	G_{p3} (MSCF)	N_p (STB)	Z (Frac)	Z_2 (Frac)	V_o (Frac)
1	3,224	0.000	0.000	0.000	0.000	0.858	0.858	0.000
2	3,000	52.617	1.299	0.211	8.390	0.864	0.851	0.124
3	2,750	114.455	2.544	0.413	16.291	0.868	0.843	0.152
4	2,500	178.810	3.647	0.592	23.162	0.872	0.836	0.157
5	2,250	245.214	4.641	0.754	29.246	0.876	0.828	0.156
6	2,000	313.246	5.551	0.902	34.711	0.882	0.820	0.151
7	1,750	382.486	6.397	1.040	39.691	0.889	0.811	0.145
8	1,500	452.499	7.199	1.170	44.314	0.897	0.800	0.139
9	1,250	522.826	7.982	1.298	48.714	0.907	0.785	0.131
10	1,000	592.971	8.778	1.427	53.066	0.919	0.764	0.124
11	750	662.361	9.641	1.568	57.651	0.932	0.730	0.116
12	500	730.220	10.690	1.740	63.061	0.947	0.668	0.107

Table 12 Output from Walsh and Towler algorithm

j	G_p (MSCF)	V_o (RB)	n_T	V_g (RB)	n_g	Δn_g	$n_g/\Delta n_g$ (Frac)	ΔG_p (MSCF)	ΔN_p (STB)
1	0.000	0.000	1.000	1,018.7	1.000	0.000		0.000	0.000
2	54.127	126.432	0.938	892.2	0.810	0.062	13.166	54.127	8.390
3	117.412	154.45	0.868	864.21	0.716	0.070	10.181	63.286	7.901
4	183.05	160.34	0.796	858.32	0.643	0.072	8.961	65.637	6.871
5	250.61	158.88	0.723	859.78	0.577	0.073	7.897	67.560	6.084
6	319.70	154.26	0.649	864.40	0.512	0.074	6.915	69.090	5.465
7	389.92	148.10	0.574	870.55	0.448	0.075	5.987	70.223	4.981
8	460.87	141.14	0.499	877.52	0.383	0.075	5.095	70.946	4.622
9	532.11	133.71	0.424	884.95	0.319	0.075	4.228	71.237	4.400
10	603.18	125.94	0.348	892.72	0.254	0.075	3.376	71.070	4.353
11	673.57	117.77	0.274	900.88	0.189	0.075	2.532	70.394	4.585
12	742.65	108.85	0.199	909.80	0.126	0.074	1.687	69.079	5.410

j	G (MSCF)	N (STB)	G_{fg} (MSCF)	N_{fg} (STB)	G_{fo} (MSCF)	N_{fo} (STB)	B_o (RB/STB)	B_g (RB/MSCF)	R_s (SCF/STB)	R_v (STB/MMSCF)
1	849.55	173.01	849.55	173.01	0.000	0.000		1.20		203.65
2	795.42	164.62	712.62	110.46	82.803	54.162	2.33	1.25	1,528.81	155.00
3	732.14	156.72	644.30	80.44	87.840	76.279	2.02	1.34	1,151.56	124.85
4	666.50	149.85	588.16	61.574	78.341	88.272	1.82	1.46	887.50	104.69
5	598.94	143.76	533.49	48.042	65.449	95.720	1.66	1.61	683.76	90.05
6	529.85	138.30	477.78	37.789	52.071	100.508	1.53	1.81	518.08	79.09
7	459.63	133.32	420.43	29.819	39.203	103.498	1.43	2.07	378.78	70.93
8	388.68	128.69	361.46	23.550	27.222	105.14	1.34	2.43	258.91	65.15
9	317.45	124.29	301.17	18.602	16.278	105.69	1.27	2.94	154.01	61.77
10	246.38	119.94	239.94	14.695	6.433	105.25	1.20	3.72	61.12	61.24
11	175.98	115.36	178.24	11.609	−2.256	103.75	1.14	5.05	−21.74	65.13
12	106.90	109.95	116.55	9.128	−9.652	100.819	1.08	7.81	−95.74	78.32

References

Coats KH (1985) Simulation of gas condensate reservoir performance. JPT 5:1870

Izgec B, Barrufet MA (2005) Performance analysis of a modified black-oil model for a rich gas condensate reservoir. Paper 2005-018 presented at the Canadian International Petroleum Conference of the Petroleum Society, Calgary, Alberta

Jhaveri BS, Youngren GK (1988) Three-parameter modification of the Peng–Robinson equation of state to improve volumetric predictions. SPERE 3(3):1033–1040

Lee AL, Gonzalez MH, Eakin BE (1966) The viscosity of natural gases. J Petrol Technol 18(8):997–1000

Lohrenz J, Bray BG, Clark CR (1964) Calculating viscosities of reservoir fluids from their compositions. J Petrol Technol 16(10):1171–1176

McCain WD Jr (1990) The properties of petroleum fluid, 2nd edn. PennWell, Tulsa

Michelsen ML (1982) The isothermal flash problem. Part I. Stability. Fluid Phase Equilib 9(1):1–198

Nagy Z, Shirkovskiy AI (1982) Mathematical simulation of natural gas condensation processes using the Peng–Robinson equation of state. SPE paper 10982 presented at the 57th annual fall technical conference and exhibition of the society of petroleum engineers

Peng DY, Robinson DB (1976) A new two-constant equation of state. Ind Eng Chem Fundam 15(1):59–64

Rachford HH, Rice JD (1952) Procedure for use of electronic digital computers in calculating flash vaporization hydrocarbon equilibrium. J Petrol Tech 4(10):19, 3. Also Paper SPE-952327-G. http://dx.doi.org/10.2118/952327-G

Vardcharragosad P (2011) Field performance analysis and optimization of gas condensate systems using zero-dimensional reservoir models. MS Thesis, Pennsylvania State University, State College, Pennsylvania

Walsh MP, Lake LW (2003) A generalized approach to primary hydrocarbon recovery. Elsevier, Amsterdam

Walsh MP, Towler BF (1995) Method computes PVT properties for gas condensates. Oil Gas J 93(31):83–86

Whitson CH, Brule MR (2000) Phase behavior. SPE monograph series, vol 20. SPE, Richardson

Whitson CH, Torp SB (1983) Evaluating constant-volume depletion data. J Petrol Technol 35(3):610–620